Deterministic Inversion – Overdue for Retirement?

Ashley Francis, Managing Director
Earthworks Environment & Resources Ltd,
Prestex House, Edison Road, Churchfields, Salisbury, Wiltshire, SP2 7NU
Tel: 01722 343990

http://www.sorviodvnvm.co.uk

Limitations of Deterministic Inversion

Seismic Inversion tools designed to estimate impedance have been available to Geophysicists for over twenty years. Most of the available methods are based on minimising the difference between the seismic trace and the forward convolution of the solution with the estimated wavelet. Whether generalised linear inversion, sparse spike or simulated annealing, all the algorithms work on this basic principle of minimisation. Methods based on minimisation are commonly referred to as "deterministic".

Seismic data is bandlimited. In particular, it does not contain low frequencies and therefore absolute impedances cannot be recovered directly from the seismic trace. All inversion schemes with an absolute impedance output require a low frequency model or constraint. The low frequency scalar is usually obtained from interpolation of well data, stacking velocities or a combination of these. After inversion the low frequency model is embedded in the deterministic inversion. Artefacts in the low frequency model manifest themselves as equivalent artefacts in the deterministic inversion. An example from Francis and Syed (2001) is shown in Figure 1. Some inversion schemes amount to little more than a relative impedance (from the seismic) added to a low frequency model. This can be easily demonstrated by filtering the low frequency out of the inversion result and comparing with relative impedance. An example is shown in Figure 2. A commercial sparse spike inversion algorithm has been used to compute absolute elastic impedance (figure 2(a). By applying a low pass filter, the low frequency model is obtained (Figure 2(b)). Similarly, a high pass filter reveals the inversion contribution (Figure 2(c)) which should be compared to the relative elastic impedance obtained by zero phasing and then integrating the seismic traces (Figure 2(d)). Apart from a slight smoothing effect the sparse spike inversion result is almost indistinguishable from the relative impedance.

The value of inversion is in the well matching, wavelet estimation and deconvolution to zero phase. By integrating the seismic traces output from these processes we obtain relative impedance which is not contaminated with the artefacts often caused by efforts to obtain absolute impedance by including a low frequency constraint.

Minimisation techniques together with the bandwidth limitations have some side-effects which are not always appreciated by end users of inversion products. Firstly, minimisation results in the output impedance distribution having a smaller variance than the actual impedance observed at the wells. This means it is inappropriate to apply well log derived cutoffs (eg to indicate the presence or absence of sands) to the results of inversion as the estimates will be biased. An example is shown in Figure 3 where a trace from a conventional inversion (using both kriged and deterministic model generation methods) midway between two wells (Wells 8 and 10 along xline155 in the Stratton 3D seismic data). Note the reduced range of impedance compared to the well values. Sands are indicated by higher impedances, above 8150 (see Francis, 1997). The deterministic inversion would suggest 7% sand proportion but the wells show the sand proportion to be 19%. The two wells are just

800 m apart. Methods based on minimising differences in trace amplitudes (ie reflectivity) have the additional problem that the resulting distribution of impedances will have skewed errors due to the exponential transform involved in recovering impedance from reflectivity. Low impedances are over-estimated more than high impedances are underestimated.

Secondly, seismic inversion is an averaging process, caused both by the minimisation and by the bandwidth limitations. To correctly recover the reflection coefficient series we require an inverse operator which, when convolved with the estimated wavelet, will convert it to a spike (Dirac delta function). For a bandlimited wavelet, there is no operator that can give this result, instead we obtain a bandlimited spike or averaging function. Deterministically, we cannot do better than this. (Oldenburg, 1983).

Another way of looking at the band-limitation problem is to consider that in the inversion, we can add anything to the modelled reflection coefficient series which is outside of the wavelet bandwidth and it will have no effect on the match to the seismic trace. A good example of this is shown in Figure 4, where inversion has been carried out with two initial models. One model has impedance values which are twice that of the other. The impedance results appear identical until the colour scales are examined. The forward convolution of either of these impedance results yields identical synthetic traces. If we attempt to model reflectivity outside of the wavelet bandwidth we then have an arbitrary and unconstrained solution whose values depend on the algorithm, not on the rocks.

Inversion in a Stochastic Framework

One of the most common constraints used in inversion is to provide an initial model. The model is commonly an interpolation of the wells, often constrained by interpreted horizons and possibly incorporating stacking velocity data. Depending on the inversion method, this then forms some kind of initial guess or constraint.

In stochastic terms, the seismic trace is only sensitive to variations in impedance. Due to the lack of frequencies it does not contain any information about the expected value (absolute value) of impedance. In geostatistics, we would estimate the expected value away from well control using the Kriging estimator. The idea of using an initial model obtained by Kriging of well data, rather than some other, possibly sub-optimal, estimation procedure is not new. In practise, the result of inverting using a kriged model is very similar to the result obtained by using an initial model obtained using other interpolation routines.

The real insight that stochastic theory brings to seismic inversion is the concept of realisations, whose mean or average is the expected value. A simple example would be to toss a fair coin whose sides are denoted 0 or 1 for heads or tails. The expected value for any toss of the coin is 0.5, which is not a possible outcome. The outcomes, or realisations, of tossing the coin will be 0 or 1.

The idea of generating realisations of impedance, each constrained such that their forward convolution is an acceptable match to the seismic trace has been implemented by a number of authors. Haas and Dubrule (1994) pioneered a method based on sequential Gaussian simulation where an impedance trace is simulated and its derived reflectivity then convolved with the wavelet. The resulting synthetic trace is compared to the seismic trace at the same location and either accepted (if the match is good) or rejected. Debeye, Sabbah and van der Made (1996) proposed a more general method of simulation but obtain convergence with the seismic constraint via simulated annealing.

The general limitations of any stochastic seismic inversion methods are the disk space requirement (an output impedance cube is generated for each realisation) and the speed of the convergence algorithm. Accept/reject and simulated annealing methods are crude, brute force methods of convergence and generally slow.

I present here an example using an alternative approach which is a simplification of full stochastic inversion. Our method is a hybrid which we refer to as multi-point stochastic inversion or MPSI and is an extension of conventional inversion. We make the assumption that the key uncertainty is that pertaining to the low frequency model. Our stochastic impedance realisations are built such that we can incorporate this key uncertainty using conditional simulation, but obtain convergence using any conventional inversion algorithm. As a consequence our approach retains most of the benefits of stochastic inversion but without the performance disadvantage of requiring accept/reject or simulated annealing methods in order to condition to the seismic data

The method is completely general and can be derived using any stochastic method, including object and multipoint geostatistics as well as SGS or SIS, and can also incorporate co-simulations of velocity and density terms, thus allowing coupled models for both acoustic and elastic impedance inversion.

The MPSI hybrid stochastic inversion method is demonstrated on a crossline taken from the Stratton 3D dataset. The initial model has been constructed in 3D in the time domain using 14 wells within the 3D cube. Backus upscaling tests have been undertaken on the logs in order to obtain the best tie for wavelet estimation. Initial well ties are made using a phase independent amplitude envelope method. Wavelet estimation uses the Roy White method. (White, 1980; Walden and White, 1984). Both deterministic and fifty stochastic impedance results have been generated. The algorithm used in this example is generalised linear inversion, but other methods such as sparse spike can also be used. The deterministic inversion result is shown in Figure 5 and four of the impedance realisations are shown in Figure 6.

The increased variability is shown with the impedance trace midway between wells 10 and 8 (see Figure 7). The range of impedance is closer to the well range and significantly wider than the deterministic inversion. The stochastic inversion traces have a sand proportion of 18.8%, very close to the 19.0% observed in the two wells. A summary of the impedance statistics and sand proportion predicted is given in the table shown in Figure 7. The effect of applying an impedance cutoff to denote sand is demonstrated on both the deterministic and the stochastic results, illustrating the bias introduced by deterministic methods.

Finally, Figure 9 shows a sand prediction based on > 8150 impedance values. On the left of Figure 9 is the sand indicator from deterministic inversion. Note the lack of sand indicated in the 400-450ms interval. On the right is the sand probability determined from 50 stochastic inversion results. Note the high probability of sand extending from the 10 well to the 8 well in the 400-450ms interval.

References

Oldenburg, D.W., Scheuer, T. And Levy, S., 1983, Recovery of the acoustic impedance from reflection seismograms. *Geophysics* 48 (10) pp 1318-1337

Debeye, H.W.J., Sabbah, E. and van der Made, P.M., 1996, Stochastic Inversion. Presented at 65th Annual International SEG meeting, Denver, USA.

Francis, A.M., 1997, Acoustic impedance inversion pitfalls and some fuzzy analysis. *The Leading Edge*, March 1997, pp275-278

Francis, A.M. and Syed, F.H., 2001, Application of relative acoustic impedance inversion to constrain extent of E sand reservoir on Kadanwari Field. Presented at SPE/PAPG Annual Technical conference, 7-8 November 2001, Islamabad, Pakistan.

White, R. E., 1980, Partial coherence matching of synthetic seismograms with seismic traces. *Geophysical Prospecting* 28 pp 333-358

Walden, A.T. and White, R.E., 1984, On errors of fit and accuracy in matching synthetic seismograms and seismic traces. *Geophysical Prospecting* 32 pp 871-891

Figures

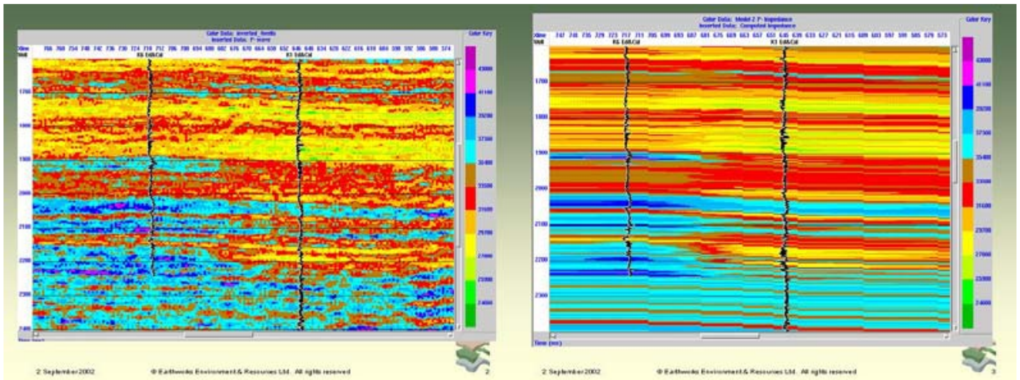

Figure 1 Comparison of inversion result (left) with initial model (right) showing how artefacts from well interpolation causes artefacts in the inversion. The reservoir sands (impedances shown as yellow/green in the interval 2150-2200ms) appear to deteriorate between the K1 and K6 wells (left). The culprit is the interpolation method used to create the initial model (right). From Francis and Syed (2001).

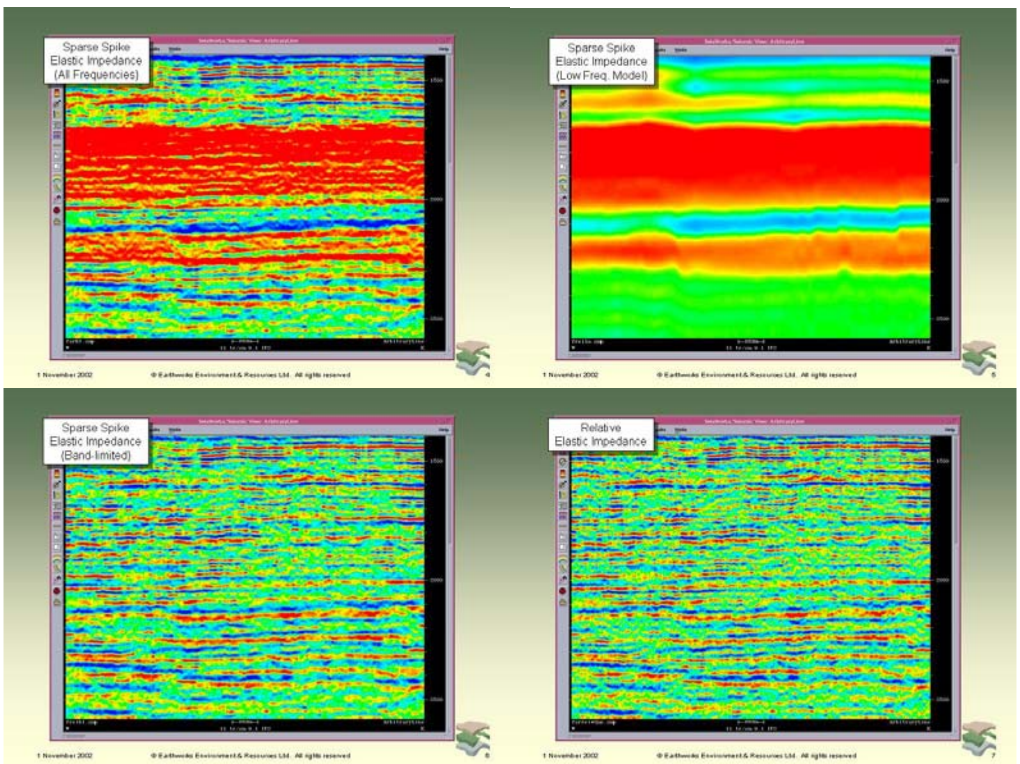

Figure 2 (a) A commercial sparse spike inversion algorithm has been used to compute absolute elastic impedance (top left)). (b) By applying a low pass filter, the low frequency model is obtained (top right). (c) A high pass filter reveals the inversion contribution (lower left) which should be compared to (d) the relative elastic impedance obtained by zero phasing and then integrating the seismic traces (lower right).

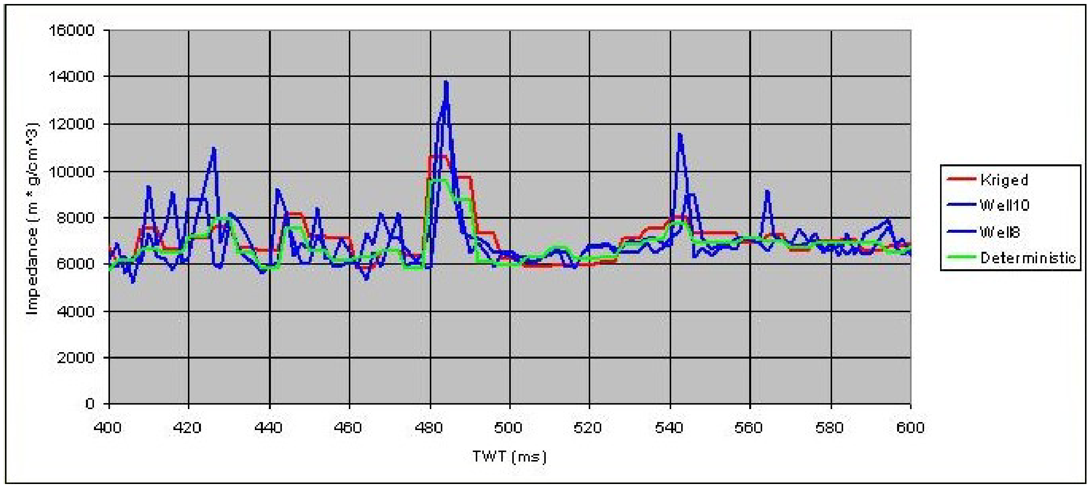

Figure 3 A trace from a conventional inversion (kriged and deterministic) midway between wells 8 and 10. Note the reduced range of impedance compared to the well values. Sands are indicated by higher impedances, above 8150. The deterministic inversion would suggest 7% sand proportion but the wells show the sand proportion to be 19%. The two wells are just 800 m apart.

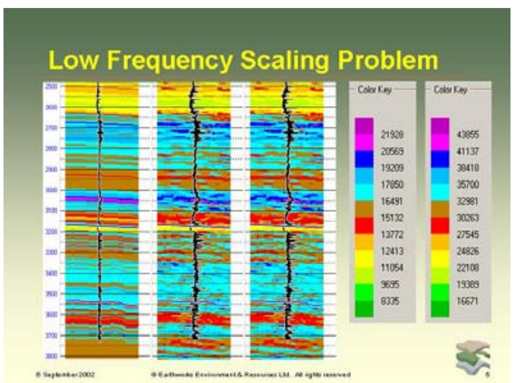

Figure 4 Inversion run twice with the same model but scaled by a factor of 2. The model is at left, then the two inversions. Their colour tables are shown to the right.

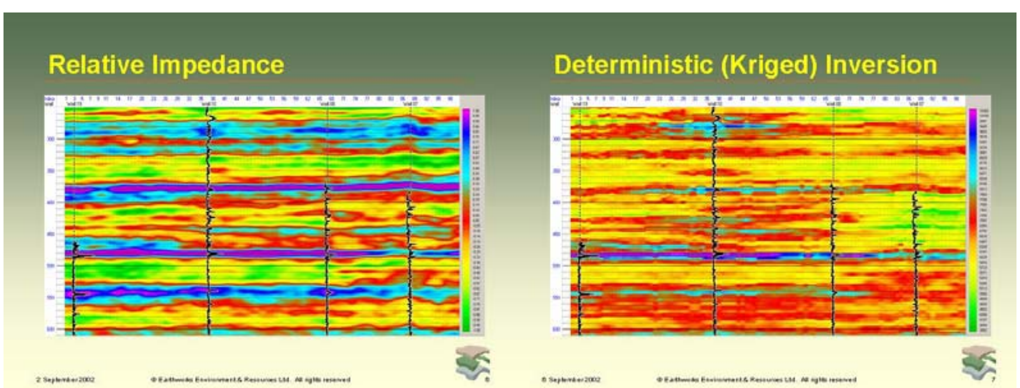

Figure 5 Relative impedance (left) and deterministic inversion based on a kriged 3D initial model (right)

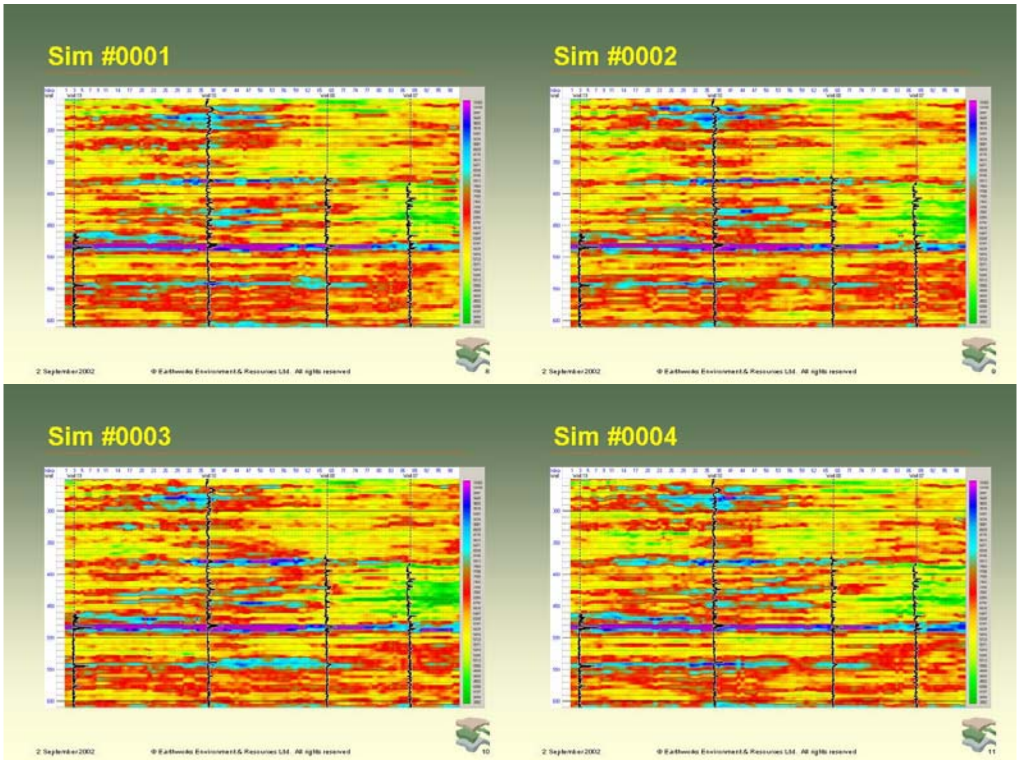

Figure 6 Four realisations using the new hybrid stochastic inversion.

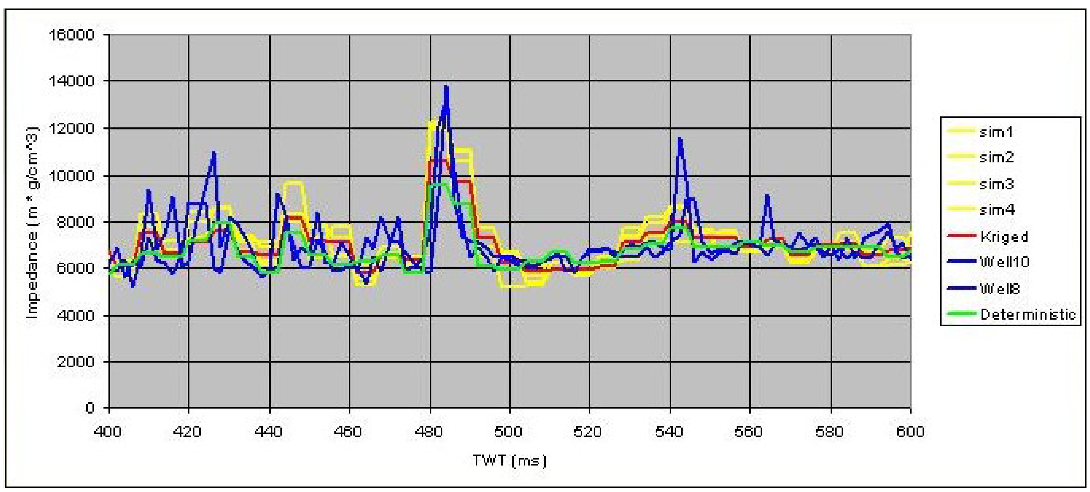

Figure 7 4 realisation traces midway between wells 10 and 8 overlaid on the data of Fig 2. Note the range of impedance is closer to the well range and significantly wider than the deterministic inversion. The stochastic inversion traces have a sand proportion of 19.0%, the same as observed in the two wells.

Comparison of Results

	Deterministic	Kriged	Sims	Wells
Min	5634	5816	5360	5262
Mean	7013	7336	7354	7292
Max	9555	10573	12102	13556
SD	841	929	1155	1316
Net	6.9%	15.7%	18.8%	19.0%

Figure 8 Table of results showing how the stochastic inversions more closely reproduce the impedance variation observed in the wells. As a consequence the proportion of sand is accurately recovered by analysing the realisations.

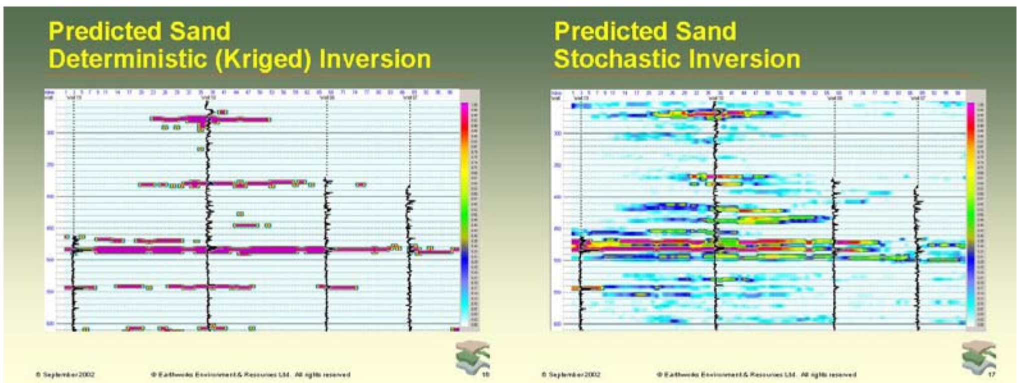

Figure 9 Sand prediction based on > 8150 impedance values. At left is sand indicator from deterministic inversion. Note lack of sand indicated in the 400-450ms interval. On the right is the sand probability determined from 50 stochastic inversion results. Note the high probability of sand extending from the 10 well to the 8 well in the 400-450ms interval.